Desalination and Water Treatment
www.deswater.com
doi: 10.5004/dwt.2023.29194

283 (2023) 97–108
January

A comprehensive study on the effect of variation of flow rate of fluid and N on energy metrics of N similar photovoltaic thermal flat plate collectors integrated single slope solar still

Gaurav Kumar Sharma[a], Ashis Mallick[a], R.K. Sharma[b], Navneet Kumar[c], Desh Bandhu Singh[d,*]

[a]*Department of Mechanical Engineering, Indian Institute of Technology (ISM), Dhanbad, Jharkhand, India, emails: kavi.me.siet@gmail.com (G.K. Sharma), mal123_us@yahoo.com (A. Mallick)*
[b]*University of Petroleum and Energy Studies (UPES), Bidholi, Premnagar, Dehradun – 248007, Uttarakhand, India, email: ram.sharma@upes.ac.in*
[c]*Department of Mechanical Engineering, Maharana Pratap Polytechnic, Gorakhpur, Uttar Pradesh - 273015, India, email: navneet.mech48@gmail.com*
[d]*Department of Mechanical Engineering, Graphic Era Deemed to be University, Bell Road, Clement Town, Dehradun – 248002, Uttarakhand, India, email: deshbandhusingh.me@geu.ac.in/dbsiit76@gmail.com*

Received 9 July 2022; Accepted 9 December 2022

ABSTRACT

This paper communicates an analysis on the influence of variation of flow rate of fluid ($\dot{m}_f$) and number of collectors (N) on energy metrics for N alike PVT flat plate collectors integrated single slope solar still (N-PVTFPCSS) at constant water depth for sustainable solar distillation. N-PVTFPCSS has the potential to fulfill the sustainable development goal of United Nations. The computation of energy metrics for various values of $\dot{m}_f$ and N has been done using computer code written in MATLAB-2015a considering all the four climatic conditions in each month of New Delhi. The evaluation has been carried out for a year. It is deduced that value of energy payback time for N-PVTFPCSS at given water depth of 0.14 m enhances with the enhancement in $\dot{m}_f$ at given N and becomes almost constant beyond 0.10 kg/s. The optimum value of N for energy metrics comes out to be 6 from energy viewpoint and 8 from exergy viewpoint.

Keywords: Energy metrics; Flow rate of fluid; N; Active solar still; Exergy; PVT

1. Introduction

The analysis of solar still which is solely based on solar energy and it does not create any pollutants which may harm the environment. The working of solar still is based on greenhouse effect. Also, solar still is self-sustainable in most of the cases and it can be set up in distant locations for providing clean water for numerous purposes including drinking for human beings after mixing some minerals to distilled water. It can provide clean water to the community without disturbing the environment and in this way, it helps in achieving the sustainable development goals of United Nations. A lot of developments have been carried out throughout the world. The active solar still (ACSS) was experimented by Rai and Tiwari [1] in 1983 in which one flat plate collector (FPC) was included with single slope solar still (SS) and it was deduced that output of freshwater was higher than the conventional solar still (CSS) because of the provision of heat to basin by FPC. However, the system was not self-sustainable. So, Kumar and Tiwari [2] performed experimental investigation by integrating FPC

* Corresponding author.

and PVT for providing heat to basin of SS. The idea was taken from the findings reported by Kern and Russell [3]. They stated that the electrical efficiency increased due to passing of fluid below PVT. Kumar and Tiwari [2] deduced an improvement in freshwater yield by 3.5 times as compared to CSS due to the presence of collectors which absorb heat from sunlight and transfers the same to basin. This work was further lengthened by Singh et al. [4] for double slope solar still (DS). Singh et al. [5] and Tiwari et al. [6] performed experimental study of SS incorporated with two identical PVTFPCs. They found an improvement in electrical energy over the system of Kumar and Tiwari [2] due to increased area of PVT.

ACSS was investigated for optimized values of flow rate of fluid ($\dot{m}_f$) and N at constant water depth [7–11]. It was deduced that ACSS of DS form provided an improved energy payback time (ENPT) over CSS by 74.66%. The value of exergy output per unit cost for ACSS was obtained as 47.37% more than CSS having same basin area. The use of nanofluid was presented by Sahota et al. [12] in ACSS of DS kind for boosting the freshwater yield. Carranza et al. [13] studied DS having nanofluid and also included the preheating of saline water. It was deduced that freshwater yield increased because of better thermophysical characteristic of nanofluid over base fluid. Kouadri et al [14] have studied ACSS having zinc and copper oxides as nanoparticles in base fluid and deduced that freshwater yield was higher by 79.39% than CSS.

Atheaya et al. [15] reported PVT integrated compound parabolic concentrator collector (CPC) with the objective of getting higher output as concentrator could concentrate more solar energy on the receiver surface. This work was further lengthened by Tripathi et al. [16] for getting characteristic equations for N similar series connected PVTCPCs. Singh and Tiwari [17–19], Gupta et al. [20,21], Singh et al. [22,23] and Sharma et al. [24] studied solar stills by incorporating development of equations and deduced that ACSS of DS type performed better than ACSS under optimized values of $\dot{m}_f$ and N at constant value of water depth because of improved allocation energy obtained from sunlight in ACSS of DS form. Prasad et al. [25], Bharti et al. [26], Singh [27] made sensitivity study for ACSS of DS form and deduced that the analysis could help the designer and installer of solar still as they could have information in advance about the effect of input parameters on the output.

The performance of solar collector used in ACSS could be improved by using evacuated tubes as convective heat loss would be prevented using such tubes. Sampathkumar et al. [28] studied ACSS containing evacuated tubular collector and stated that the output of clean water was improved over CSS having basin area equal to that of ACSS by 129% due to collection of heat from sunlight by collectors and transferring the same to basin. Singh et al. [29] investigated solar desalting unit including evacuated tubes (ETs) and working under natural circulation mode. They concluded that the exergy efficiency was in the range of 0.15% to 8%. Further, a study on ACSS involving ETs was carried out in forced mode and an improved performance was obtained as compared to natural circulation mode because of improved circulation of fluid [30]. Mishra et al. [31] developed fundamental equations for evacuated tubular collectors (ETCs) which were linked in series. An extended version of their work was studied by Singh et al. [32] and Singh and Tiwari [33,34]. They reported fundamental equations development for series connected N-ETCs to basin type solar still and compared single and double slope ACSS considering exergo-enviro-economic parameters and energy metrics. An extended version of the work done by Singh et al. was further studied by Issa and Chang [35] in which ETCs were linked as mixed mode and concluded that the performance was enhanced over passive mode operated solar still because of the provision of heat to basin in ACSS. Furthermore, Singh and Al-Helal [36], Singh et al. [37] and Sharma et al. [38,39] developed fundamental equations for ACSS by connecting solar still with N-ETCs as well as concentrator integrated ETC.

Patel et al. [40–42] reviewed ACSS involving different sorts of collectors and reported the effect of various designs of collectors on the performance of ACSS. Further, Singh et al. [43] performed short review on ACSS containing nanofluid and stated that the performance of nano-fluid loaded solar stills was better because of the improved properties of nanofluid. A comparison of ETCs integrated solar stills in natural and forced modes were carried out by Shankar et al. [44]. They reported that the forced mode operated solar still was better in terms of carbon credit earned. Sharma et al. [45] reviewed renewable energy system loaded with nanofluid-based heat transfer by incorporating machine learning aspect and concluded that the addition of small amount of solid particles on nano size having high thermal conductivity enhanced the heat transfer rate and resulted in the performance of the system. Said et al. [46] investigated ionic liquid-MXene hybrid nanofluid experimentally and concluded that the reported nanofluid could be used in solar systems for getting better output. Jeevadason et al. [47] reviewed solar still containing nano-fluid from exergo-enviro-economic analyses viewpoint and they concluded that the nanofluid loaded hybrid solar system performed better because of the improved thermophysical property. Further, Shoeibi et al. [48] reviewed solar still having heat pipe and they concluded that there was a significant improvement in the output if heat pipe was used. Said et al. [49] studied the evaluation of specific heat capacity of nanofluid using machine learning techniques.

The current literature survey reveals that the effect of dissimilarity of mass flow rate ($\dot{m}_f$) and number of collectors (N) on energy metrics for N alike PVT flat plate collectors integrated single slope solar still (N-PVTFPCSS) has not been carried out by any investigator all over the world. For knowing the effect of $\dot{m}_f$ and N on energy metrics of N-PVTFPCSS, all 4 types of weather conditions have been taken into account. Some works on energy metrics of N-PVTFPCSS have been carried out, however, they are different from the current work. The difference being that the current work focuses on the estimation of variation of $\dot{m}_f$ and N on energy metrics, whereas, in previous work, energy metrics for the ACSS had been carried out at some chosen values of $\dot{m}_f$ and N.

2. Working of N-PVTFPCSS

The set-up of N-PVTFPCSS and its specification has been revealed as Fig. 1 and Table 1, respectively. When sunlight

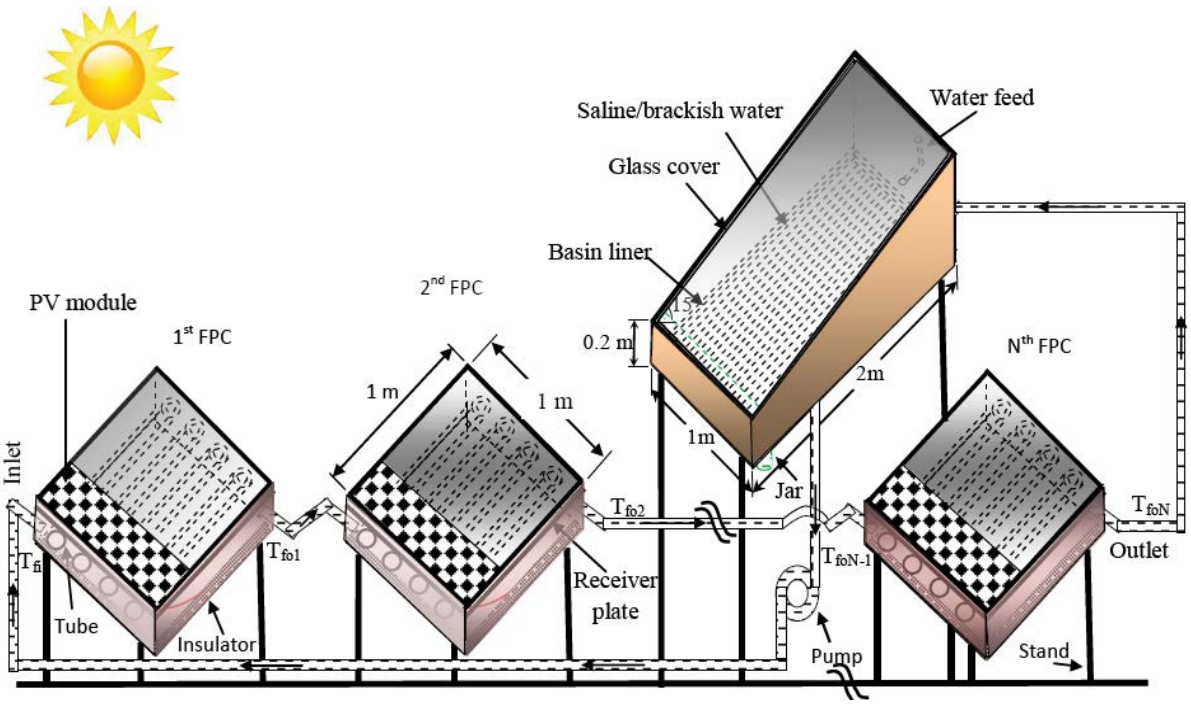

Fig. 1. Schematic diagram of N-PVTFPCSS.

Table 1
Specifications of N-PVTFPCSS

Solar still of single slope type			
Component	Specification	Component	Specification
Length	2 m	Orientation	South
Width	1 m	Thickness of glass cover	0.004 m
Inclination of glass cover	15°	k_g	0.816 W/m-K
Height of smaller side	0.2 m	Thickness of insulation	0.1 m
Material of body	GRP	Thermal conductivity of insulation	0.166 W/m-K
Material of stand	GI	Cover material	Glass

PVT-FPC collector			
Component	Specification	Component	Specification
Type and no of collectors	Tube in plate type, N	Area of module	0.25 m × 1.0 m
Receiver area of solar water collector	1.0 m × 1.0 m	Area of collector	0.75 m × 1.0 m
Collector plate thickness	0.002	F'	0.968
Thickness of copper tubes	0.00056 m	ρ	0.84
Length of each copper tubes	1.0 m	τ_g	0.95
K_i (Wm/K)	0.166	α_c	0.9
FF	0.8	β_c	0.89
Thickness of insulation	0.1 m	α_p	0.8
Angle of FPC with horizontal	30°	Pipe diameter	0.0125 m
Thickness of toughen glass on FPC	0.004 m	DC motor rating	12 V, 24 W
Effective area of collector under glass	0.75 m²		

falls on the surface of solar still, some part gets reflected, some part is absorbed, and the remaining part is transmitted to water surface. At the water surface, some part is again reflected, some part is absorbed by water and the remaining part is transmitted to the blackened surface where almost all radiation gets absorbed. The temperature of blackened surface rises and it transmits heat to water. N-PVTFPCs connected to basin also provides heat and temperature of

water rises. Water gets evaporated due to temperature difference between water surface and the condensing surface. The vapor gets condensed at the inside surface of condensing cover and trickles down due to gravity. The fresh water is then siphoned off to the measuring flask.

3. Fundamental equations used for the analysis of N-PVTFPCSS

The fundamental equations used for the analysis of N-PVTFPCSS is developed by writing energy balance equations for the various components of N-PVTFPCSS followed by the simplification of these equations using the concept of mathematics. The fundamental equations used for the analysis of N-PVTFPCSS are as follows:

The useful heat gain from N-PVTFPCs can be computed as [50] as:

$$\dot{Q}_{uN} = N\left(A_m + A_c\right)\left[\left(\pm\ddot{A}\right)_{\text{eff},N} I(t) - U_{L,N}\left(T_{fi} - T_a\right)\right] \tag{1}$$

In the proposed system, N-PVTFPCs is in closed loop with basin of solar still. Water coming from the basin enters the first PVTFPC using DC motor pump and the outlet from Nth PVTFPC is again allowed to go to the basin for increasing temperature of basin. The temperature of water coming out from N-PVTFPC (T_{foN}) can be estimated as [50]:

$$T_{foN} = \frac{\left(\text{AF}_R(\alpha\tau)\right)_1}{\dot{m}_f C_f}\frac{\left(1-K_k^{\,N}\right)}{\left(1-K_k\right)} I(t) + \frac{\left(AF_R U_L\right)_1}{\dot{m}_f C_f}\frac{\left(1-K_k^{\,N}\right)}{\left(1-K_k\right)} T_a + K_k^{\,N} T_{fi} \tag{2}$$

where $T_{fi} = T_w$. Eqs. (1) and (2) have many unknown terms that has been given in Appendix A.

The electrical efficiency of solar cells (η_{cN}) for N-PVTFPCSS can be written as [51,52]:

$$\eta_{cN} = \eta_0\left[1 - \beta_0\left(\overline{T}_{cN} - T_0\right)\right] \tag{3}$$

In Eq. (3), η_o represents efficacy for standard condition, $\overline{T}_{cN}$ represents mean temperature of cell. The value of $\overline{T}_{cN}$ has been estimated using relation reported in Shyam et al. [46] taking $T_{fi} = T_w$ as N-PVTFPCs forms a closed loop with basin.

After rearranging energy balance equations for several parts of SS and making use of Eq. (1), the relation for water temperature (T_w) can be obtained in the form of a function of time as [5,6]:

$$T_w = \frac{\overline{f}_1(t)}{a_1}\left(1 - e^{-a_1 t}\right) + T_{w0} e^{-a_1 t} \tag{4}$$

where T_{w0} stands for initial value of T_w, $\overline{f}_1(t)$ stands for mean value of $f_1(t)$ for the considered small time interval.

Once T_w has been known and it can be evaluated making use of Eq. (4), temperature of inner and outer surface of glass cover (T_{gi} and T_{go}) can be presented as:

$$T_{gi} = \frac{\alpha_g' I_s(t) A_g + h_{1w} T_w A_b + U_{c,ga} T_a A_g}{U_{c,ga} A_g + h_{1w} A_b} \tag{5}$$

$$T_{go} = \frac{\frac{K_g}{L_g} T_{gi} + h_{1g} T_a}{\frac{K_g}{L_g} + h_{1g}} \tag{6}$$

After knowing the relations for T_w and T_{gi}, one can find the hourly clean water production ($\dot{m}_{ew}$) as:

$$\dot{m}_{ew} = \frac{h_{ewg} A_b\left(T_w - T_{gi}\right)}{L} \times 3600 \tag{7}$$

Here, L is latent heat and its value has been considered as 2,400 kJ/kg-K in the current work.

The relation for electrical energy $\left(\dot{E}x_e\right)$ produced by N-PVTFPCSS can be given as follows:

$$\dot{E}x_e = A_m I_b(t) \sum_1^N \left(\alpha\tau_g \eta_{cN}\right) \tag{8}$$

4. Analysis

The climatic condition used for the analysis of N-PVTFPCSS can be characterized by number of sunshine hours (N') and ratio of daily diffuse to daily global irradiation (r') [53]. If values of r' and N' are respectively less than or equal to 0.25 and greater than or equal to 9 h, the climate is known as clear day. If the range of r' is from 0.25 to 0.5 and the range of N' is from 7 h to 9 h, the climate is known as hazy day. If the range of r' is from 0.50 to 0.75 and the range of N' is from 5 h to 7 h, the climate is known as hazy and cloudy. If values of r' and N' are respectively greater than or equal to 0.25 and less than or equal to 9 h, the climate is known as cloudy.

4.1. Energy and exergy computations

The expression of yearly overall energy (E_{out}) and yearly overall exergy ($G_{ex,annual}$) for N-PVTFPCSS considering 1st and 2nd laws of thermodynamics can be written as:

$$E_{out} = \frac{\left(M_{ew} \times L\right)}{3600} + \frac{\left(P_m - P_u\right)}{0.38} \tag{9}$$

$$G_{ex,annual} = h_{ewg} \times \frac{A_b}{2} \times \left[\begin{array}{c}\left(T_w - T_{gi}\right) - (T_a + 273) \\ \times \ln\left\{\frac{(T_w + 273)}{\left(T_{gi} + 273\right)}\right\}\end{array}\right] + \left(P_m - P_u\right) \tag{10}$$

where M_{ew} is annual freshwater yield, P_m is annual electrical power generated, P_u represents yearly consumption of pump and L represents latent heat. The factor 0.38 [51] in

Eq. (9) changes electrical energy into heat. The first term on right hand side of Eq. (10) has been taken from Nag [54]. The evaporative heat transfer coefficient (h_{ewg}) can be estimated as:

$$h_{ewg} = 16.273\times10^{-3} h_{cwg}\left[\frac{P_w - P_{gi}}{T_w - T_{gi}}\right] \text{ [55]} \tag{11}$$

$$h_{c,wg} = 0.884\left[\left(T_w - T_{gi}\right) + \frac{\left(P_w - P_{gi}\right)\left(T_w + 273\right)}{268.9\times10^3 - P_w}\right]^{\left(\frac{1}{3}\right)} \text{ [56]} \tag{12}$$

$$P_w = \exp\left[25.317 - \frac{5144}{\left(T_w + 273\right)}\right] \tag{13}$$

And

$$P_{gi} = \exp\left[25.317 - \frac{5144}{\left(T_{gi} + 273\right)}\right] \tag{14}$$

4.2. Energy metrics estimation

It is an important part for solar energy-oriented systems because energy metrics gives information about the viability of N-PVTFPCSS from energy as well as exergy consideration. The term energy metrics comprises of three terms namely energy payback time (ENPT), energy production factor (EPRF) and life cycle conversion efficiency (LICCE). Energy metrics considers the entire life of the system while evaluating different parameters. The embodied energy includes energy as well as exergy and the exergy part is much higher. Lower value of embodied energy should be selected for the system to be economical. For the calculation of embodied energy, energy density of all the components needs to be focused. The embodied energy of the component can be computed as the product of mass of the component and energy density of that component's material. Then, the addition of embodied energies for all components of the renewable energy system results in the embodied energy of the system.

4.2.1. ENPT estimation

The time needed to retrieve the embodied energy of the renewable energy system is known as ENPT. Its value can be computed based on energy and exergy both. Here, one should note that exergy based ENPT has greater value than energy based ENPT because exergy represents the quality of energy and hence the value of exergy is much lower than the value of energy output. Lower the value of ENPT, better is the system as less time will be required to achieve the breakeven point and it will also result in the higher amount of carbon credited. ENPT for N-PVTFPCSS can be computed as [57]:

$$\text{ENPT}_{energy} = \frac{\text{Embodied energy of NPVTFPC} - \text{SS}\left(E_{in}\right)}{\text{Annual energy output obtained from NPVTFPC} - \text{SS}\left(E_{out}\right)} \tag{15}$$

$$\text{ENPT}_{exergy} = \frac{\text{Embodied energy of NPVTFPC} - \text{SS}}{\text{Annual energy output obtained from NPVTFPC} - \text{SS}\left(E_{out}\right)} \tag{16}$$

The value of hourly exergy rate can be estimated as follows:

$$\text{Hourly exgy} = h_{ewg}\times A\times\left[\frac{\left(T_w - T_{gi}\right) + \left(T_a + 273\right)}{\ln\left\{\frac{\left(T_w + 273\right)}{\left(T_{gi} + 273\right)}\right\}}\right] \tag{17}$$

4.2.2. EPRF estimation

EPRF is the reciprocal of ENPT. Values of EPRF for N-PVTFPCSS can be computed as:

$$\text{EPRF}_{energy} = \frac{\text{Annual energy output obtained from } N - \text{PVTFPCSS}\left(E_{out}\right)}{\text{Embodied energy of } N - \text{PVTFPCSS}\left(E_{in}\right)} \tag{18}$$

$$\text{EPRF}_{,exergy} = \frac{\text{Annual energy output obtained from } N - \text{PVTFPCSS}\left(E_{out}\right)}{\text{Embodied energy of } N - \text{PVTFPCSS}\left(E_{in}\right)} \tag{19}$$

4.2.3. LICCE estimation

It gives an idea about the net output of the solar energy system with respect to solar energy falling on the system. It is distinct from efficiency. The difference lies in the fact that LICCE deems the whole life of N-PVTFPCSS. Its ideal value is one. Higher the value of LICCE, better is the system. The value of LICCE can be computed as:

$$\text{LICCE}_{energy} = \frac{\left(\text{Annual energy}\times n\right) - E_{in}}{\left(\text{Annual solar exergy}\right)\times n} \tag{20}$$

$$\text{LICCE}_{exergy} = \frac{\left(\text{Annual exergy}\times n\right) - E_{in}}{\left(\text{Annual solar exergy}\right)\times n} \tag{21}$$

5. Solution procedure

The solution procedure for knowing the effect of variation of $\dot{m}_f$ and N on energy metrics of N-PVTFPCSS are as follows:

Step I

The required input data for solar flux on horizontal surface and ambient temperature has been accessed from

IMD Pune, India. The value of solar flux on the inclined surface has been estimated using Liu and Jordan formula by computer code in MATLAB.

Step II

Eq. (7) has been used for the computation of hourly fresh water yielding for various values of $\dot{m}_f$ and N followed by gross energy computation using Eq. (9). Further, Eq. (10) has been used for the computation of gross exergy output from the system.

Step III

Eqs. (15) and (16) have been used for the estimation of ENPT followed by the estimation of EPRF using Eqs. (18) and (19). Further, LICCE has been estimated using Eqs. (20) and (21).

6. Results and discussion

All needed information and expressions have been provided input to the computational code written in MATLAB 2015a. Data accessed from IMD Pune for the horizontal surface has also been obtained for the inclined surface taking Liu and Jordan formula into consideration using computer code in MATLAB. The output so obtained has been depicted as Figs. 2–10 and Tables 2 and 3.

Eq. (7) has been used to estimate the hourly fresh water yielding followed by the calculation of daily, monthly and yearly fresh water yielding. During the calculation of monthly clean water production for various values of $\dot{m}_f$ and N, four different kinds of weather situations mentioned in analysis section have been used. After evaluation of net monthly yield, yearly yield for different values of $\dot{m}_f$ and N has been estimated as the addition of monthly yield for 12 months and they have been presented as Fig. 2. Further, Eq. (9) has been used to estimate values of annual total energy output for various values of $\dot{m}_f$ and N for system under consideration. For evaluating these values, computer code written in MATLAB 2015a has been used and they have been presented as Fig. 3.

Eq. (10) has been used to estimate values of annual gross exergy output for various values of $\dot{m}_f$ and N for the system under consideration. For evaluating these values, computer code written in MATLAB 2015a has been used and they have been presented as Fig. 4. It can be seen in Fig. 4 that the value of gross exergy output diminishes with the increase in value of $\dot{m}_f$ and value of gross exergy output ceases to vary beyond $\dot{m}_f$ = 0.01 kg/s. The reason behind the diminish in the value of gross exergy can be attributed to less time available for gaining heat from sunlight for the fluid passing through tubes of collector at increased speed. When the speed becomes further higher, the fluid just glides through collector without absorbing heat and no further heat is added to the basin water.

The estimation of embodied energy for several components of system has been depicted as Table 2. The embodied energy has been evaluated for the particular component as the multiplication of energy density of the material of that component and the mass of the component. This way, embodied energy for all components has been evaluated and finally embodied energies for all components have been added for getting the embodied energy for N-PVTFPCSS. The calculation of the amount of solar energy striking the surface of intended system has been depicted as Table 3. It is observed that value of solar energy increases with the increases in the value of N because area of the system increases with the increase in the value of N. Based on the literature review, it has been assumed that the intended system works properly for 30 y.

The variation of ENPT on the basis of energy with $\dot{m}_f$ for N-PVTFPCSS at different N has been depicted in Fig. 5. One can clearly see in Fig. 5 that value of ENPT for the intended system increases as value of $\dot{m}_f$ is increased at given N. It is also observed that value of ENPT almost ceases to vary

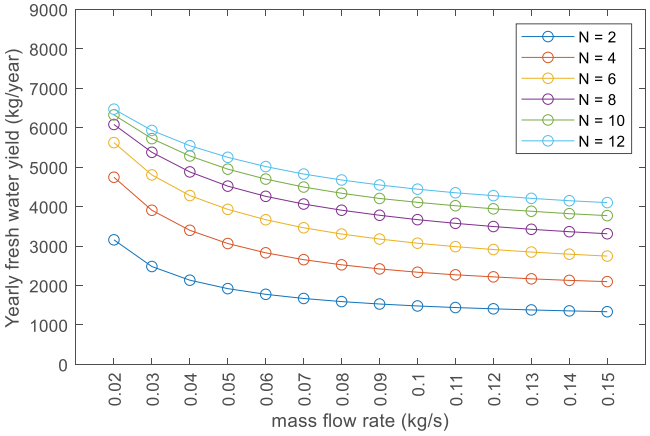

Fig. 2. Variation of yearly clean water production with $\dot{m}_f$ and N for N-PVTFPCSS.

Table 2
Embodied energy computation for N-PVTFPCSS

Component	Embodied energy					
	$N = 2$	$N = 4$	$N = 6$	$N = 8$	$N = 10$	$N = 12$
Solar still of single slope type	1,737.79	1,737.79	1,737.79	1,737.79	1,737.79	1,737.79
Flat plate collector	1,104.96	2,209.92	3,314.88	4,419.84	5,524.8	6,629.76
PVT	490	980	1470	1,960	2,450	2,940
Others	20	20	20	20	20	20
Total (kWh)	3,352.75	4,947.71	6,542.67	8,137.63	9,732.59	11,327.55

Table 3
Solar energy computation for N-PVTFPCSS for life span of 30 y

Component	Solar energy					
	$N = 2$	$N = 4$	$N = 6$	$N = 8$	$N = 10$	$N = 12$
Solar still of single slope type	116,882.7	116,882.7	116,882.7	116,882.7	116,882.7	116,882.7
PVTFPC	222,671.5	445,343.1	668,014.6	890,686.1	1,113,358	1,336,029
Solar energy (kWh)	339,554.2	562,225.8	784,897.3	1,007,569	1,230,240	1,452,912

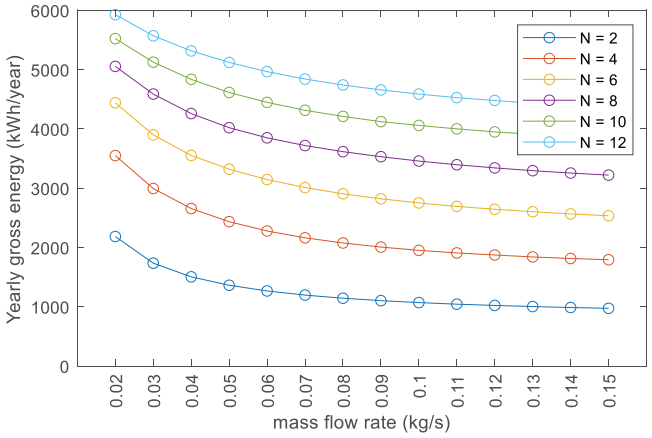

Fig. 3. Dissimilarity of annual gross energy output with $\dot{m}_f$ and N for N-PVTFPCSS.

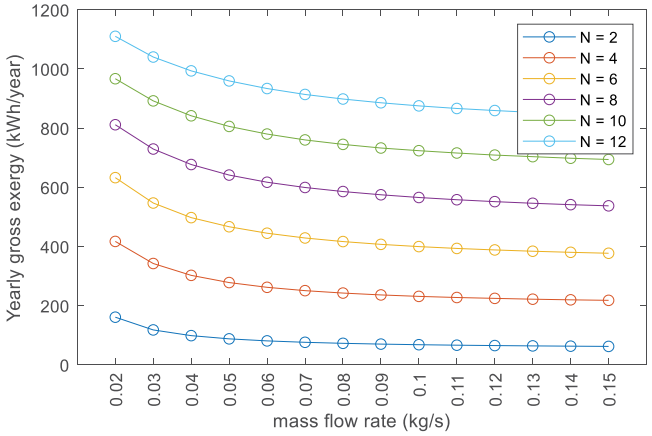

Fig. 4. Dissimilarity of annual gross exergy with $\dot{m}_f$ and N for N-PVTFPCSS.

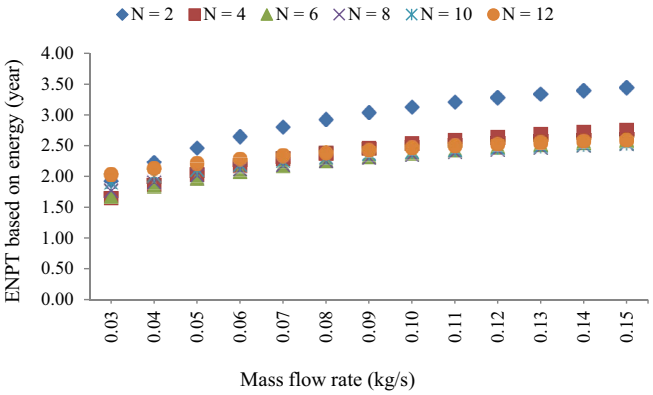

Fig. 5. Dissimilarity of ENPT based on energy with $\dot{m}_f$ and N for NPVFPC-SS.

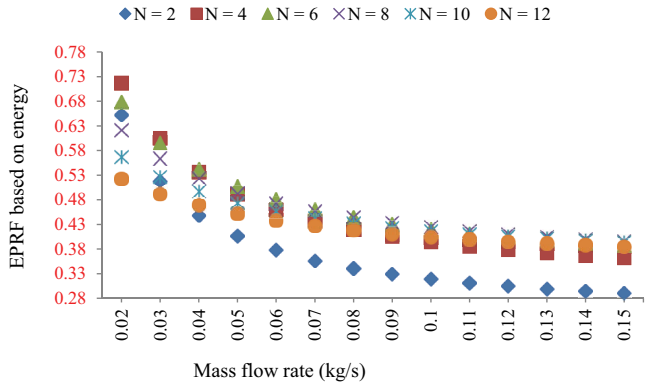

Fig. 6. Variation of EPRF based on energy with $\dot{m}_f$ and N for N-PVTFPCSS.

beyond 0.10 kg/s. It has been found to occur because water flowing through collector does not find time to absorb energy at enhanced value of $\dot{m}_f$. It is further observed that the optimum value of N for N-PVTFPCSS from energy based ENPT is 6 as the value of ENPT becomes either constant beyond $N = 6$ or increases. The variation of EPRF on the basis of energy with $\dot{m}_f$ for N-PVTFPCSS at different N has been revealed as Fig. 6. The expression of EPRF is reciprocal of ENPT. So, higher the value of EPRF better is the system. The optimum value of N from EPRF viewpoint comes out to be 6 as the value of EPRF beyond $N = 6$ remains either constant or diminish. It is further observed from Fig. 6 that the value of EPRF diminishes with the enhancement in $\dot{m}_f$ value because water does not get sufficient time to absorb heat from solar energy while passing through collectors. Beyond $\dot{m}_f$ = 0.1 kg/s, the value of EPRF remains almost constant because heated water does not get further heated due to very low value of temperature difference between water flowing through collector tubes and its surroundings.

The variation of LICCE on the basis of energy with $\dot{m}_f$ for N-PVTFPCSS at different N has been depicted in Fig. 7. It is seen in Fig. 7 that value of LICCE lessens as the value of $\dot{m}_f$ increase as diminished energy output is obtained which further happens due to diminished heat addition by collector to the basin of solar still at enhanced values of $\dot{m}_f$ because water flowing through collector does not find time to collect heat from solar energy. Beyond

$\dot{m}_f$ = 0.10 kg/s, values of LICCE based on energy become almost constant due to similar behavior in energy output obtained from the system at enhanced values of $\dot{m}_f$. It is seen in Fig. 7 that the optimal value of N is 6 because value of LICCE remains either constant or diminishes beyond N = 6.

The variation of ENPT on the basis of exergy with $\dot{m}_f$ for N-PVTFPCSS at different N has been depicted in Fig. 8. One can see in Fig. 8 that the value of exergy based ENPT for N-PVTFPCSS enhances with the increase in value of $\dot{m}_f$ at given N and the value of exergy based ENPT for N-PVTFPCSS becomes almost constant beyond 0.10 kg/s. It occurs because exergy gain diminishes with the enhancement in value of $\dot{m}_f$ which further happens due to lower temperature of water in the basin at enhanced values of $\dot{m}_f$ as heat absorbed by water flowing through collector is diminished with the enhancement in value of $\dot{m}_f$. It is further observed that the optimal value of N for N-PVTFPCSS from exergy based ENPT viewpoint is 8 as the value of exergy based ENPT becomes constant beyond N = 8.

The variation of EPRF on the basis of exergy with $\dot{m}_f$ for N-PVTFPCSS at different N has been revealed as Fig. 9. The exergy based EPRF is reciprocal of exergy based ENPT. So, higher the value of exergy based EPRF better is the system. The optimal value of N has been obtained as 8 from viewpoint of EPRF based on exergy because value of EPRF beyond N = 8 remains constant. It is further observed from Fig. 8 that the value of EPRF based on exergy diminishes with the increase in $\dot{m}_f$ value because time available for water to absorb heat is low and hence water is not able to absorb heat from solar energy while passing through collectors which results in lower temperature rise of water in basin and hence lower exergy output. Beyond $\dot{m}_f$ = 0.1 kg/s, the value of exergy based EPRF remains almost constant because heated water does not get further heated due to very low value of temperature difference between water flowing through collector tubes and its surroundings.

The variation of LICCE on the basis of exergy with $\dot{m}_f$ for N-PVTFPCSS at different N has been depicted in Fig. 10. One can see in Fig. 10 that the value of LICCE based on exergy decreases with the increase in $\dot{m}_f$ value for all values of N and value of LICCE based on exergy becomes almost constant beyond $\dot{m}_f$ = 0.10 kg/s. It is also clear from Fig. 10 that the system is not feasible from exergy viewpoint for $N \leq 2$ as the value of exergy based LICCE comes out to be negative. The optimum value of N from exergy-based LICCE viewpoint comes out to be 8 as the value of exergy based LICCE beyond N = 8 become almost constant. It occurs due to the fact that the heated water does not get further heated due to lower temperature difference between water flowing through collectors and the surroundings.

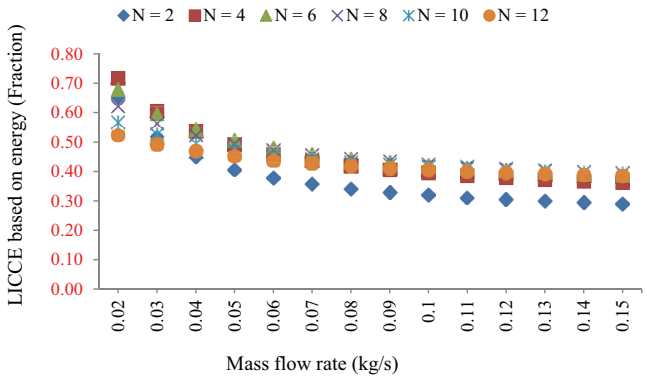

Fig. 7. Variation of LICCE based on energy with $\dot{m}_f$ and N for N-PVTFPCSS.

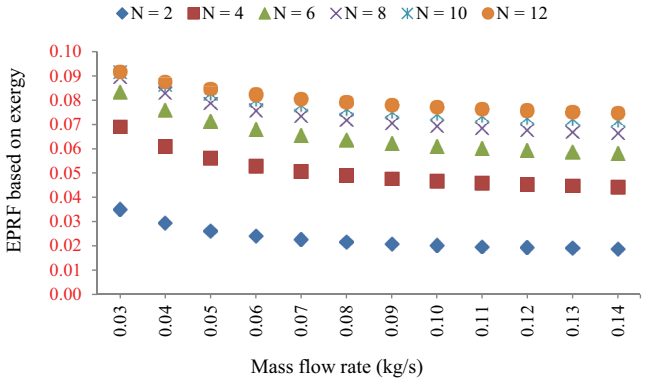

Fig. 9. Variation of EPRF based on exergy with $\dot{m}_f$ and N for N-PVTFPCSS.

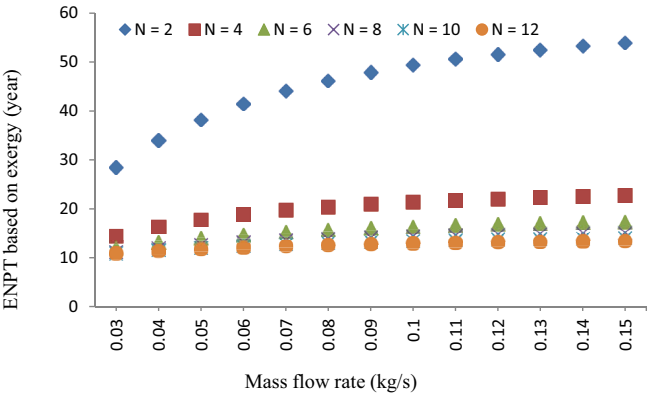

Fig. 8. Variation of ENPT based on exergy with $\dot{m}_f$ and N for N-PVTFPCSS.

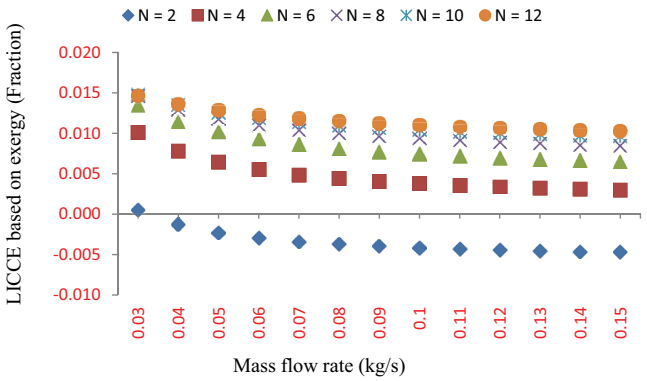

Fig. 10. Dissimilarity of LICCE based on exergy with $\dot{m}_f$ and N for N-PVTFPCSS.

7. Conclusions

The current research focuses on finding out the effect of variation of $\dot{m}_f$ and N on energy matrices of N-PVTFPCSS considering all four kinds of weathers. Based on the current research, the following conclusions can be drawn:

- The value of ENPT based on energy and exergy has been found to diminish with the increase in values of $\dot{m}_f$ and it becomes almost constant beyond $\dot{m}_f$ = 0.10 kg/s. The optimum value of N has been obtained as 6 and 8 respectively for energy and exergy based ENPT.
- The value of EPRF based on energy and exergy has been found to diminish with the increase in values of $\dot{m}_f$ and it becomes almost constant beyond $\dot{m}_f$ = 0.10 kg/s. The optimum value of N has been obtained as 6 and 8 respectively for energy and exergy based ENPT.
- From the viewpoint of exergy based LICCE, it is found that N-PVTFPCSS is not feasible if $N \leq 2$. The optimal value of N has been obtained as 6 for energy based LICCE and 8 for exergy based LICCE.

8. Recommendations

Results of the system will be very useful for the designer and installer of the system as the effect of mass flow rate and number of collectors on the performance will be known in advance to them. The effect of geographical location on the performance of the active solar still has not been reported. Authors would like to work upon the effect of geographical location on the performance of the active solar still and the same will be reported in the next research paper. The effect of hybrid nanofluid has also not been reported.

Symbols

A_m — Area covered by PV module, m²
A_c — Area covered by glass, m²
A_g — Area of glass cover, m²
A_b — Area of basin, m²
L — Latent heat, J/kg
L_g — Thickness of glass cover, m
K_g — Thermal conductivity of glass, W/m-K
$I(t)$ — Global radiation falling on collector, W/m²
T_a — Ambient temperature, °C
L_i — Thickness of insulation, m
K_i — Thermal conductivity of insulation, W/m-K
α_c — Absorptivity of the solar cell
$\dot{m}_f$ — Mass flow rate of water, kg/s
τ_g — Transmissivity of the glass, fraction
C_f/C_w — Specific heat of water, J/kg-K
β_o — Temperature coefficient of efficiency, K⁻¹
L_c — Length of collector covered by glass
L_m — Length of collector covered by PV module
η_c — Solar cell efficiency
η_m — PV module efficiency
η_{cN} — Temperature dependent electrical efficiency of solar cells of a NPVTFPCs
b — Breath of collector, m
$(\alpha\tau)_{eff}$ — Product of effective absorptivity and transmittivity
F' — Collector efficiency factor
T_c — Solar cell temperature, °C
T_p — Absorber plate temperature, °C
L_p — Thickness of absorber plate, m
K_p — Thermal conductivity of absorber plate, W/m-K
T_{fi} — Fluid temperature at collector inlet, °C
T_f — Temperature of fluid in collector, °C
PF_1 — Penalty factor due to the glass covers of module
PF_2 — Penalty factor due to plate below the module
PF_3 — Penalty factor due to the absorption plate for the glazed portion
PF_c — Penalty factor due to the glass covers for the glazed portion
β — Packing factor of the module
η_o — Efficiency at standard test condition
T_{foN} — Outlet water temperature at the end of Nth PVTFPC water collector, °C
h_i — Heat transfer coefficient for space between the glazing and absorption plate, W/m²-K
h'_i — Heat transfer coefficient from bottom of PVT to ambient, W/m²-K
h_o — Heat transfer coefficient from top of PVT to ambient, W/m²-K
U_{tca} — Overall heat transfer coefficient from cell to ambient, W/m²-K
U_{tcp} — Overall heat transfer coefficient from cell to plate, W/m²-K
h_{pf} — Heat transfer coefficient from blackened plate to fluid, W/m²-K
U_{tpa} — Overall heat transfer coefficient from plate to ambient, W/m²-K
U_{Lm} — Overall heat transfer coefficient from module to ambient, W/m²-K
U_{Lc} — Overall heat transfer coefficient from glazing to ambient, W/m²-K
P_m — Annual power generated from photovoltaic module, kWh
P_u — Annual power utilized by pump, kWh
ϵ — Emissivity
α' — Absorptivity
$\dot{E}x$ — Hourly exergy, W
$I_S(t)$ — Solar intensity on glass cover of solar still of single slope type, W/m²
T_{gi} — Glass temperature at inner surface of glass cover, °C
h_{rwg} — Radiative heat transfer coefficient from water to inner surface of glass cover, W/m²-K
h_{cwg} — Convective heat transfer coefficient from water to inner surface of glass cover, W/m²-K
h_{ewg} — Evaporative heat transfer coefficient, W/m²-K
M_w — Mass of water in basin, kg
$\dot{m}_{ew}$ — Mass of distillate from of double slope solar still, kg
a — Clear days, blue sky
b — Hazy days, fully

c — Hazy and cloudy days, partially
d — Cloudy days, fully
$\dot{Q}_{uN}$ — Rate of useful thermal output from N identical partially (25%) covered PVTFPC water collectors connected in series, kWh
$G_{ex,annual}$ — Annual exergy gain, kWh
ln — Natural logarithm
SS — Single slope
t — Time, h
T_s — Temperature of sun, °C
T_w — Temperature of water in basin, °C
T_a — Ambient temperature, °C
T_{wo} — Water temperature at t = 0, °C
$\overline{T}_{CN}$ — Average solar cell temperature
E_{out} — Overall annual energy available from PVT-CPC solar distillation system, kWh
N — Number of PVTFPC water collector
E_{in} — Embodied energy, kWh
FPC — Flat plate collector
PVT — Photovoltaic thermal
GRP — Glass reinforced plastic
ACSS — Active solar still
DS — Double slope solar still
PVTFPC — Photovoltaic thermal flat plate collector
ENPT — Energy payback time
ET — Evacuated tube
ETC — Evacuated tubular collector
ρ — Reflectivity
N-PVTFPCSS — N identical PVTFPC integrated single slope solar still
FF — Fill factor
T_{go} — Temperature at outer surface of glass, °C
EPRF — Energy production factor
LICCE — Life cycle conversion efficiency
N' — Number of sunshine hours
T_{EPB} — Energy payback time
F_{EP} — Energy production factor
η_{LCC} — Life cycle conversion efficiency
r' — Daily diffuse to daily global irradiation ratio

Subscripts

g — Glass
w — Water
in — Incoming
out — Outgoing
eff — Effective

References

[1] S.N. Rai, G.N. Tiwari, Single basin solar still coupled with flat plate collector, Energy Convers. Manage., 23 (1983) 145–149.
[2] S. Kumar, A. Tiwari, An experimental study of hybrid photovoltaic thermal (PV/T) active solar still, Int. J. Energy Res., 32 (2008) 847–858.
[3] E.C. Kern, M.C. Russell, Combined Photovoltaic and Thermal Hybrid Collector Systems, Proceedings of the 13th IEEE Photovoltaic Specialists, June 5–8, Washington, D.C., USA, pp. 1153–1157.
[4] G. Singh, S. Kumar, G.N. Tiwari, Design, fabrication and performance of a hybrid photovoltaic/thermal (PVT) double slope active solar still, Desalination, 277 (2011) 399–406.
[5] D.B. Singh, J.K. Yadav, V.K. Dwivedi, S. Kumar, G.N. Tiwari, I.M. Al-Helal, Experimental studies of active solar still integrated with two hybrid PVT collectors, Sol. Energy, 130 (2016) 207–223.
[6] G.N. Tiwari, J.K. Yadav, D.B. Singh, I.M. Al-Helal, AM. Abdel-Ghany, Exergoeconomic and enviroeconomic analyses of partially covered photovoltaic flat plate collector active solar distillation system, Desalination, 367 (2015) 186–196.
[7] D.B. Singh, G.N. Tiwari, Enhancement in energy metrics of double slope solar still by incorporating N identical PVT collectors, Sol. Energy, 143 (2017) 142–161.
[8] D.B. Singh, Exergoeconomic and enviroeconomic analyses of N identical photovoltaic thermal integrated double slope solar still, Int. J. Exergy, 23 (2017) 347–366.
[9] D.B. Singh, N. Kumar, Harender, S. Kumar, S.K. Sharma, A. Mallick, Effect of depth of water on various efficiencies and productivity of N identical partially covered PVT collectors incorporated single slope solar distiller unit, Desal. Water Treat., 138 (2019) 99–112.
[10] D.B. Singh, Improving the performance of single slope solar still by including N identical PVT collectors, Appl. Therm. Eng., 131 (2018) 167–179.
[11] D.B. Singh, N. Kumar, S. Kumar, V.K. Dwivedi, J.K. Yadav, G.N. Tiwari, Enhancement in exergoeconomic and enviroeconomic parameters for single slope solar still by incorporating N Identical partially covered photovoltaic collectors, J. Sol. Energy Eng., 140 (2018) 051002 (18 pages), doi: 10.1115/1.4039632.
[12] L. Sahota, G.N. Tiwari, Exergoeconomic and enviroeconomic analyses of hybrid double slope solar still loaded with nanofluids, Energy Convers. Manage., 148 (2017) 413–430.
[13] F. Carranza, C. Villa, J. Aguilara, H.A. Borbón-Nuñez, D. Sauceda, Experimental study on the potential of combining TiO_2, ZnO, and Al_2O_3 nanoparticles to improve the performance of a double-slope solar still equipped with saline water preheating, Desal. Water Treat., 216 (2021) 14–33.
[14] M.R. Kouadri, N. Chennouf, M.H. Sellami, M.N. Raache, A. Benarima, The effective behavior of ZnO and CuO during the solar desalination of brackish water in southern Algeria, Desal. Water Treat., 218 (2021) 126–134.
[15] D. Atheaya, A. Tiwari, G.N. Tiwari, I.M. Al-Helal., Analytical characteristic equation for partially covered photovoltaic thermal (PVT) – compound parabolic concentrator (CPC), Sol. Energy, 111 (2015) 176–185.
[16] R. Tripathi, G.N. Tiwari, I.M. Al-Helal, Thermal modelling of N partially covered photovoltaic thermal (PVT)–compound parabolic concentrator (CPC) collectors connected in series, Sol. Energy, 123 (2016) 174–184.
[17] D.B. Singh, G.N. Tiwari, Performance analysis of basin type solar stills integrated with N identical photovoltaic thermal (PVT) compound parabolic concentrator (CPC) collectors: a comparative study, Sol. Energy, 142 (2017) 144–158.
[18] D.B. Singh, G.N. Tiwari, Exergoeconomic, enviroeconomic and productivity analyses of basin type solar stills by incorporating N identical PVT compound parabolic concentrator collectors: a comparative study, Energy Convers. Manage., 135 (2017) 129–147.
[19] D.B. Singh, G.N. Tiwari, Effect of energy matrices on life cycle cost analysis of partially covered photovoltaic compound parabolic concentrator collector active solar distillation system, Desalination, 397 (2016) 75–91.
[20] V.S. Gupta, D.B. Singh, R.K. Mishra, S.K. Sharma, G.N. Tiwari, Development of characteristic equations for PVT-CPC active solar distillation system, Desalination, 445 (2018) 266–279.
[21] V.S. Gupta, D.B. Singh, S.K. Sharma, N. Kumar, T.S. Bhatti, G.N. Tiwari, Modeling self-sustainable fully-covered photovoltaic thermal-compound parabolic concentrators connected to double slope solar distiller, Desal. Water Treat., 190 (2020) 12–27.
[22] V. Singh, D.B. Singh, N. Kumar, R. Kumar., Effect of number of collectors (N) on life cycle conversion efficiency of single slope solar desalination unit coupled with N identical partly covered compound parabolic concentrator collectors, Mater. Today Proc., 28 (2020) 2185–2189.

[23] D.B. Singh, G. Singh, N. Kumar, P.K. Singh, R. Kumar, Effect of mass flow rate on energy payback time of single slope solar desalination unit coupled with N identical compound parabolic concentrator collectors, Mater. Today Proc., 28 (2020) 2551–2556.
[24] G.K. Sharma, N. Kumar., D.B. Singh, A. Mallick, Exergoeconoic analysis of single slope solar desalination unit coupled with PVT-CPCs by incorporating the effect of dissimilarity of the rate of flowing fluid mass, Mater. Today Proc., 28 (2020) 2364–2368.
[25] H. Prasad, P. Kumar, R.K. Yadav, A. Mallick, N. Kumar, D.B. Singh, Sensitivity analysis of N identical partially covered (50%) PVT compound parabolic concentrator collectors integrated double slope solar distiller unit, Desal. Water Treat., 153 (2019) 54–64.
[26] K. Bharti, S. Manwal, C. Kishore, R.K. Yadav, P. Tiwar, D.B. Singh, Sensitivity analysis of N alike partly covered PVT flat plate collectors integrated double slope solar distiller unit, Desal. Water Treat., 211 (2021) 45–59.
[27] D.B. Singh, Sensitivity analysis of N identical evacuated tubular collectors integrated double slope solar distiller unit by incorporating the effect of exergy, Int. J. Exergy, 34 (2021) 424–447.
[28] K. Sampathkumar, T.V. Arjunan, P. Senthilkumar, The experimental investigation of a solar still coupled with an evacuated tube collector, Energy Sources Part A, 35 (2013) 261–270.
[29] R.V. Singh, S. Kumar, M.M. Hasan, M.E. Khan, G.N. Tiwari, Performance of a solar still integrated with evacuated tube collector in natural mode, Desalination, 318 (2013) 25–33.
[30] S. Kumar, A. Dubey, G.N. Tiwari, A solar still augmented with an evacuated tube collector in forced mode, Desalination, 347 (2014) 15–24.
[31] R.K. Mishra, V. Garg, G.N. Tiwari, Thermal modeling and development of characteristic equations of evacuated tubular collector (ETC), Sol. Energy, 116 (2015) 165–176.
[32] D.B. Singh, V.K. Dwivedi, G.N. Tiwari, N. Kumar, Analytical characteristic equation of N identical evacuated tubular collectors integrated single slope solar still, Desal. Water Treat., 88 (2017) 41–51.
[33] D.B. Singh, G.N. Tiwari, Analytical characteristic equation of N identical evacuated tubular collectors integrated double slope solar still, J. Sol. Energy Eng., 135 (2017) 051003 (11 pages), doi: 10.1115/1.4036855.
[34] D.B. Singh, G.N. Tiwari, Energy, exergy and cost analyses of N identical evacuated tubular collectors integrated basin type solar stills: a comparative study, Sol. Energy, 155 (2017) 829–846.
[35] R.J. Issa, B. Chang, Performance study on evacuated tubular collector coupled solar still in west Texas climate, Int. J. Green Energy, 14 (2017) 793–800.
[36] D.B. Singh, I.M. Al-Helal, Energy metrics analysis of N identical evacuated tubular collectors integrated double slope solar still, Desalination, 432 (2018) 10–22.
[37] D.B. Singh, N. Kumar, A. Raturi, G. Bansal, A. Nirala, N. Sengar, Effect of Flow of Fluid Mass Per Unit Time on Life Cycle Conversion Efficiency of Double Slope Solar Desalination Unit Coupled with N Identical Evacuated Tubular Collectors, R.M. Singari, K. Mathiyazhagan, H. Kumar, Eds., Lecture Notes in Mechanical Engineering, Advances in Manufacturing and Industrial Engineering, Select Proceedings of ICAPIE 2019, Springer, Singapore, 2021, pp. 393–402.
[38] S.K. Sharma, D.B. Singh, A. Mallick, S.K. Gupta, Energy metrics and efficiency analyses of double slope solar distiller unit augmented with N identical parabolic concentrator integrated evacuated tubular collectors: a comparative study, Desal. Water Treat., 195 (2020) 40–56.
[39] S.K. Sharma, A. Mallick, S.K. Gupta, N. Kumar, D.B. Singh, G.N. Tiwari, Characteristic equation development for double slope solar distiller unit augmented with N identical parabolic concentrator integrated evacuated tubular collectors, Desal. Water Treat., 187 (2020) 178–194.
[40] R.V. Patel, K. Bharti, G. Singh, R. Kumar, S. Chhabra. D.B. Singh, Solar still performance investigation by incorporating the shape of basin liner: a short review, Mater. Today Proc., 43 (2021) 597–604.
[41] R.V. Patel, K. Bharti, G. Singh, G. Mittal, D.B. Singh, A. Yadav, Comparative investigation of double slope solar still by incorporating different types of collectors: a mini review, Mater. Today Proc., 38 (2021) 300–304.
[42] R.V. Patel, G. Singh, K. Bharti, R. Kumar, D.B. Singh, A mini review on single slope solar desalination unit augmented with different types of collectors, Mater. Today Proc., 38 (2021) 204–210.
[43] G. Singh, D.B. Singh, S. Kumara, K. Bharti, S. Chhabra, A review of inclusion of nanofluids on the attainment of different types of solar collectors, Mater. Today Proc., 38 (2021) 153–159.
[44] P. Shankar, A. Dubey, S. Kumar, G.N. Tiwari, Production of clean water using ETC integrated solar stills: thermoenviro-economic assessment, Desal. Water Treat., 218 (2021) 106–118.
[45] P. Sharma, Z. Said, A. Kumar, S. Nižetić, A. Pandey, A.T. Hoang, Z. Huang, A. Afzal, C. Li, A.T. Le, X.P. Nguyen, V.D. Tran, Recent advances in machine learning research for nanofluid-based heat transfer in renewable energy system, Energy Fuels, 36 (2022) 6626–6658.
[46] Z. Said, P. Sharma, N. Aslfattahi, M. Ghodbane, Experimental analysis of novel ionic liquid-MXene hybrid nanofluid's energy storage properties: model-prediction using modern ensemble machine learning methods, J. Energy Storage, 52 (2022) 104858, doi: 10.1016/j.est.2022.104858.
[47] A. Wesley Jeevadason, S. Padmini, C. Bharatiraja, A.E. Kabeel, A review on diverse combinations and Energy-Exergy-Economics (3E) of hybrid solar still desalination, Desalination, 527 (2022) 115587, doi: 10.1016/j.desal.2022.115587.
[48] S. Shoeibi, S.A.A. Mirjalily, H. Kargarsharifabad, M. Khiadani, H. Panchal, A comprehensive review on performance improvement of solar desalination with applications of heat pipes, Desalination, 540 (2022) 115983, doi: 10.1016/j.desal.2022.115983.
[49] Z. Said, P. Sharma, R.M. Elavarasan, A.K. Tiwari, M.K. Rathod, Exploring the specific heat capacity of water-based hybrid nanofluids for solar energy applications: a comparative evaluation of modern ensemble machine learning techniques, J. Energy Storage, 54 (2022) 105230, doi: 10.1016/j.est.2022.105230.
[50] Shyam, G.N. Tiwari, I.M. Al-Helal, Analytical expression of temperature dependent electrical efficiency of N-PVT water collectors connected in series, Sol. Energy, 114 (2015) 61–76.
[51] D.L. Evans, Simplified method for predicting PV array output, Sol. Energy, 27 (1981) 555–560.
[52] T. Schott, Operational Temperatures of PV Modules, Proceedings of 6th PV Solar Energy Conference, 1985, pp. 392–396.
[53] H.N. Singh, G.N. Tiwari, Evaluation of cloudiness/haziness factor for composite climate, Energy, 30 (2005) 1589–1601.
[54] P.K. Nag, Basic and Applied Thermodynamics, Tata McGraw-Hill, ISBN 0-07-047338-2, 2004.
[55] P.I. Cooper, Digital simulation of experimental solar still data, Sol. Energy, 14 (1973) 451–456.
[56] R.V. Dunkle, Solar Water Distillation, the Roof Type Solar Still and Multi-Effect Diffusion Still, International Developments in Heat Transfer, A.S.M.E., Proceedings of International Heat Transfer, Part V(1961) 895, University of Colorado.
[57] G.N. Tiwari, R.K. Mishra, Advanced Renewable Energy Sources, Royal Society of Chemistry Publishing House, UK, ISBN 978-1-84973-380-9, 2012.

Appendix

Expressions for various terms used in Eqs. (1)–(9) are as follows.

$$U_{\text{tca}} = \left[\frac{1}{h_0} + \frac{L_g}{K_g}\right]^{-1};\ U_{\text{tcp}} = \left[\frac{1}{h_i} + \frac{L_g}{K_g}\right]^{-1};$$

$$h_0 = 5.7 + 3.8V, Wm^{-2}K^{-1}; h_i = 5.7, Wm^{-2}K^{-1};$$

$$U_{\text{tpa}} = \left[\frac{1}{U_{\text{tca}}} + \frac{1}{U_{\text{tcp}}}\right]^{-1} + \left[\frac{1}{h_i'} + \frac{1}{h_{\text{pf}}} + \frac{L_i}{K_i}\right]^{-1};$$

$$h_i' = 2.8 + 3V,\ Wm^{-2}K^{-1};$$

$$U_{L1} = \frac{U_{\text{tcp}}U_{\text{tca}}}{U_{\text{tcp}} + U_{\text{tca}}};\ U_{L2} = U_{L1} + U_{\text{tpa}};$$

$$U_{Lm} = \frac{h_{\text{pf}}U_{L2}}{F'h_{\text{pf}} + U_{L2}};\ U_{Lc} = \frac{h_{\text{pf}}U_{\text{tpa}}}{F'h_{\text{pf}} + U_{\text{tpa}}};$$

$$\text{PF}_1 = \frac{U_{\text{tcp}}}{U_{\text{tcp}} + U_{\text{tca}}};\ \text{PF}_2 = \frac{h_{pf}}{F'h_{\text{pf}} + U_{L2}};$$

$$\text{PF}_c = \frac{h_{\text{pf}}}{F'h_{\text{pf}} + U_{\text{tpa}}};\ (\alpha\tau)_{1\text{eff}} = (\alpha_c - \eta_c)\tau_g\beta_c;$$

$$(\alpha\tau)_{2\text{eff}} = \alpha_p\tau_g^2(1-\beta_c);\ (\alpha\tau)_{\text{meff}} = \left[(\alpha\tau)_{2\text{eff}} + \text{PF}_1(\alpha\tau)_{1\text{eff}}\right];$$

$$(\alpha\tau)_{\text{ceff}} = \text{PF}_c\alpha_p\tau_g;\ A_m = \text{WL}_m;\ A_c = \text{WL}_c;$$

$$A_cF_{\text{Rc}} = \frac{\dot{m}_fc_f}{U_{Lc}}1 - \exp\left(\frac{-F'U_{Lc}A_c}{\dot{m}_fc_f}\right);$$

$$A_mF_{Rm} = \frac{\dot{m}_fc_f}{U_{Lm}}1 - \exp\left(\frac{-F'U_{Lm}A_m}{\dot{m}_fc_f}\right);$$

$$\left(\text{AF}_R(\alpha\tau)\right)_1 = \left[A_cF_{Rc}(\alpha\tau)_{\text{ceff}} + PF_2(\alpha\tau)_{\text{meff}}A_mF_{Rm}\left(1 - \frac{A_cF_{Rc}U_{Lc}}{\dot{m}_fc_f}\right)\right];$$

$$\left(AF_RU_L\right)_1 = \left[A_cF_{Rc}U_{Lc} + A_mF_{Rm}U_{Lm}\left(1 - \frac{A_cF_{Rc}U_{Lc}}{\dot{m}_fc_f}\right)\right];$$

$$K_K = \left(1 - \frac{(\text{AF}_RU_L)_1}{\dot{m}_fc_f}\right);\ \left(\text{AF}_R(\alpha\tau)\right)_{m1} = \text{PF}_2(\alpha\tau)_{\text{meff}}A_mF_{Rm};$$

$$\left(\text{AF}_RU_L\right)_{m1} = A_mF_{Rm}U_{Lm};\ K_m = \left(1 - \frac{A_mF_{Rm}U_{Lm}}{\dot{m}_fc_f}\right);$$

$$(\alpha\tau)_{\text{eff},N} = \frac{\left(\text{AF}_R(\alpha\tau)\right)_1}{(A_c + A_m)}\left[\frac{1-(K_K)^N}{N(1-K_K)}\right];$$

$$U_{L,N} = \frac{(\text{AF}_RU_L)_1}{(A_c + A_m)}\left[\frac{1-(K_K)^N}{N(1-K_K)}\right]$$

$$a_1 = \frac{1}{M_wC_w}\left[\dot{m}_fC_f\left(1-K_k^N\right) + U_sA_b\right];$$

$$\overline{f_1}(t) = \frac{1}{M_wC_w}\left[\begin{array}{c}\alpha'_{\text{eff}}A_b\overline{I}_s(t) + \frac{\left(1-K_k^N\right)}{(1-K_k)}\left(\text{AF}_R(\alpha\tau)\right)_1\overline{I}_c(t)\\ +\left(\frac{\left(1-K_k^N\right)}{(1-K_k)}\left(\text{AF}_RU_L\right)_1 + U_sA_b\right)\overline{T}_a\end{array}\right];$$

$$\alpha'_{\text{eff}} = \alpha'_w + h_1\alpha'_b + h'_1\alpha'_g;\ h_1 = \frac{h_{\text{bw}}}{h_{\text{bw}} + h_{\text{ba}}};$$

$$h'_1 = \frac{h_{1w}A_g}{U_{c,\text{ga}}A_g + h_{1w}A_b};\ h_{1w} = h_{\text{rwg}} + h_{\text{cwg}} + h_{\text{ewg}};$$

$$h_{\text{ewg}} = 16.273\times10^{-3}h_{\text{cwg}}\left[\frac{P_w - P_{\text{gi}}}{T_w - T_{\text{gi}}}\right];$$

$$h_{\text{cwg}} = 0.884\left[\left(T_w - T_{\text{gi}}\right) + \frac{\left(P_w - P_{\text{gi}}\right)\left(T_w + 273\right)}{268.9\times10^3 - P_w}\right]^{\frac{1}{3}};$$

$$P_w = \exp\left[25.317 - \frac{5144}{T_w + 273}\right];\ P_{\text{gi}} = \exp\left[25.317 - \frac{5144}{T_{\text{gi}} + 273}\right];$$

$$h_{\text{rwg}} = \left(0.82\times5.67\times10^{-8}\right)\left[\begin{array}{c}\left(T_w + 273\right)^2\\ +\left(T_{\text{gi}} + 273\right)^2\end{array}\right]\left[T_w + T_{\text{gi}} + 546\right];$$

$$U_s = U_t + U_b; U_b = \frac{h_{\text{ba}}h_{\text{bw}}}{h_{\text{bw}} + h_{\text{ba}}};\ U_t = \frac{h_{1w}U_{c,\text{ga}}A_g}{U_{c,\text{ga}}A_g + h_{1w}A_b};$$

$$U_{c,\text{ga}} = \frac{\frac{K_g}{l_g}h_{1g}}{\frac{K_g}{l_g} + h_{1g}};\ h_{\text{ba}} = \left[\frac{L_i}{K_i} + \frac{1}{h_{\text{cb}} + h_{\text{rb}}}\right]^{-1};$$

$$h_{\text{cb}} + h_{\text{rb}} = 5.7Wm^{-2}K^{-1},\ h_{\text{bw}} = 250Wm^{-2}K^{-1};$$